MTF spectral-variation comparison of detector arrays used in multispectral imaging systems by speckle patterns

Alicia Fernández-Oliveras, Antonio M. Pozo and Manuel Rubiño; Departamento de Óptica, Facultad de Ciencias, Universidad de Granada; Granada, Spain

Abstract

Currently, cameras based on CCD and CMOS detector matrices offer excellent features in imaging systems if they are appropriately designed. Therefore, to investigate the suitability of the use of one or the other technology according to the specific application of the camera, the complete characterization of the different types of detectors becomes necessary.

In this work, we have analysed the quality of the images provided by different cameras by the speckle method. For this, we have comparatively studied the Modulation Transfer Function (MTF) at different wavelengths of the visible spectrum, for the detectors of a low-cost CCD video camera and of two scientific cameras (a CCD and a CMOS).

For the CCD detector of the video camera, the highest value of the MTF was reached at the lowest of the wavelengths studied. Furthermore, the differences between the MTF curves corresponding to the different wavelengths analysed become more notable as the spatial frequency increases.

In the case of scientific cameras, the behaviour of the MTF with wavelength does not present the same trend as that observed for the low-cost video camera. For each of the three wavelengths studied, the CCD detector presented MTF values higher than those of the CMOS detector.

Introduction

Cameras with imaging devices based on CCD and CMOS detector matrices [1] are being used more and more in such disparate fields of Science and Technology as Colorimetry, Illumination, and Astrophysics. Currently, both types of devices offer excellent features in imaging systems if they are appropriately designed. The consensus is that the two technologies complement each other and will coexist in the future, depending on the application involved [2-6].

Therefore, to investigate the suitability of the use of one or the other technology according to the specific application of the camera, the complete characterization of the different types of detector matrices becomes necessary.

A system is optically characterized by the modulation transfer function (MTF), the determination of which enables the image produced by the system to be evaluated from its response in spatial frequency [7, 8].

For measuring the MTF of solid-state cameras, the literature cites different methods that differ essentially in the type of target or pattern used as the object. Thus, for example, methods use bar targets [9], random targets [10, 11], canted self-imaging targets[12], interferometric fringes[13, 14].

One of the methods to measure the MTF, established in our laboratory, is based on using a laser speckle pattern as the object [15-20]. This method is suitable for analysing the detector independently of the camera lens, given that it does not require a lens to project the pattern. Furthermore, using a tunable laser source, we can characterize the device at different wavelengths, this proving indispensable in multispectral and colour-measuring applications.

Speckle is an interference phenomenon that occurs when coherent radiation is scattered from a rough surface. Several techniques can be used to generate the speckle pattern, such as different types of transmissive diffusers (ground glass [15], fused silica [16], microlens arrays [17]) or integrating spheres [18-20].

In the former case, an aperture situated in front of the integrating sphere enables us to specify the content of spatial frequencies of the speckle pattern. Two of the apertures used to date are the single-slit [18] and double-slit [19], both of which present advantages and drawbacks [20]. In this work, we have used a single-slit situated at the exit port of an integrating sphere.

It bears noting that in the works cited above, the systems analysed are based generally on scientific CCD cameras and comparisons were not made between devices of different quality or technology. Furthermore, neither was the MTF spectral-variation studied.

The aim of the present work is to apply the optical detector-characterization method, based on the measurement of the MTF with speckle patterns, to the analysis at different wavelengths of the image quality provided by different cameras.

For this, we have comparatively studied the resulting MTF curves at different wavelengths of the visible spectrum, for the detectors of a low-cost CCD video camera and of two scientific cameras (a CCD and a CMOS).

Theoretical background

The relationship between the theoretic power-spectral density known for a single-slit (PSD_{input}) and the measured power-spectral density (PSD_{output}) allows us to determine the MTF of the detector by means of the expression [18]:

$$PSD_{output}(\xi,\eta) = [MTF(\xi,\eta)]^2 PSD_{input}(\xi,\eta) \quad (1)$$

where ξ and η are the spatial frequencies corresponding to the horizontal and vertical directions x and y, respectively.

PSD_{output} is determined from the speckle pattern captured with the detector, being proportional to the squared magnitude of the Fourier transform of this speckle pattern. In the case of a rectangular single-slit, PSD_{input} is given by [21, 22]:

$$PSD_{input}(\xi,\eta) = \langle I \rangle^2 \left[\delta(\xi,\eta) + \frac{(\lambda z)^2}{l_1 l_2} tri\left(\frac{\lambda z}{l_1}\xi\right) tri\left(\frac{\lambda z}{l_2}\eta\right) \right] \quad (2)$$

where tri(X)=1-|X| for |X|≤1 and zero elsewhere; $< I >^2$ is the square of the average speckle irradiance; $\delta(\xi,\eta)$ is a delta function; l_1 and l_2 are, respectively, horizontal and vertical dimensions of the single-slit; λ is the wavelength of the laser; and z is the distance between the single-slit aperture and the detector.

Given the geometry of the single-slit, the PSD_{input} can be separated into frequencies ξ and η. The horizontal $PSD_{input}(\xi,\eta)$ is the η=0 profile of $PSD_{input}(\xi,\eta)$. This means the MTF can be determined separately for x and y directions. In the present work, we determine the horizontal MTF. This can be done in a similar way for the vertical direction.

Method

Experimental Set-up

Figure 1 presents the experimental set-up used. It is composed of a tunable ion-argon laser source (130 mW), an integrating sphere to generate the speckle pattern (inner diameter of 152.4 mm), a polarizer to provide a linearly polarized laser-speckle pattern, a single-slit (6 mm height and variable width), and an optical bench to hold the detector, which is connected to the control card installed in a personal computer.

The laser radiation is aimed at the entrance port of the integrating sphere, generating the speckle pattern at the exit port. The aperture situated at the exit port of the sphere (single-slit) determines the content in spatial frequency of the pattern registered in the detector. In these conditions, the linear polarizer ensures that the PSD_{input} is given by Eq. (2) [22].

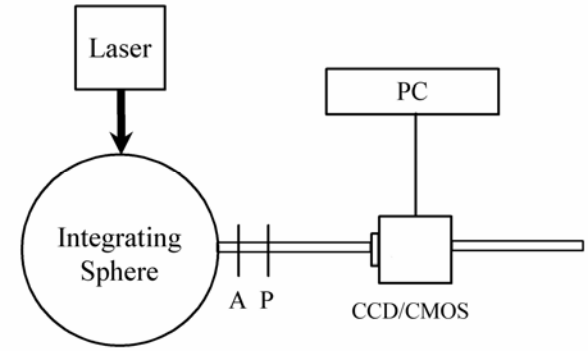

***Figure 1**. Experimental set-up for the measurement of the MTF of the detectors. The aperture A (single-slit) and the polarizer P are situated at the exit port of the integrating sphere.*

With the single-slit, the MTF can be determined from a single measurement without the need to move the detector, but it must be situated at a distance from the aperture in such a way that the maximum input spatial frequency is equal to the Nyquist frequency of the detector [16, 18]. In this way, the MTF can be determined in the largest possible frequency range, and thus aliasing is avoided.

The distance z between the detector and the single-slit aperture can be calculated by the expression:

$$z = \frac{l_1}{\lambda\, \xi_{Ny}} \tag{3}$$

where l_1 is the slit width, λ the wavelength of the laser, and ξ_{Ny} is the Nyquist spatial frequency of the detector in the horizontal direction. For a detector array with a centre-to-centre spacing between the photoelements Δx, the Nyquist frequency is given by:

$$\xi_{Ny} = \frac{1}{2\Delta x} \tag{4}$$

In this work, measurements were made using the detectors of three different cameras: a low-cost CCD video camera and two scientific cameras (a CCD and a CMOS).

The video camera was a CCD B/N Center HICB347H, connected to a Pinnacle Studio MovieBox DV control card. Its detector array is comprised of a matrix of 752x582 pixels (horizontal x vertical). The horizontal spacing between centres of these pixels is 7.98 μm, providing a Nyquist frequency of 62.66 cycles/mm in the horizontal direction by virtue of Eq. (4).

The scientific CCD camera had a high-resolution CCD B/N PixelFly array of 1360x1024 pixels with a centre-to-centre spacing between them of 4.65 μm. Consequently, with Eq. (3) taken into account, the Nyquist frequency of this detector is 107.53 cycles/mm in both directions.

The CMOS camera used was a CMOS B/N Atmos Areascan 1M30, the detector array of which had 1312x1024 pixels. In this case the pixel pitch was 5 μm in the horizontal as well as in the vertical direction, corresponding to a Nyquist frequency of 100 cycles/mm given by Eq. (3).

The width of the single-slit used was l_1=1 mm in the case of the low-cost video camera CCD detector, and l_1=3 mm for the two scientific detectors (the CCD and the CMOS).

Taking into account single-slit's width and Nyquist frequency, we can calculate the distance z between the detector and the aperture by using Eq. (3) for each wavelength studied. The corresponding values are collected in the following tables for each detector analysed.

Table 1: Distance between the detector and the single-slit aperture for the low-cost video camera CCD detector

Wavelength (nm)	Distance detector-aperture (mm)
514	31
502	32
488	33
477	33
454	35

Table 2: Distance between the detector and the single-slit aperture for scientific camera CCD detector

Wavelength (nm)	Distance detector-aperture (mm)
514	54
488	57
457	61

Table 3: Distance between the detector and the single-slit aperture for scientific camera CMOS detector

Wavelength (nm)	Distance detector-aperture (mm)
514	58
488	61
457	66

Data Processing

Once the detector was set at the corresponding distance of single-slit aperture, as indicated in the previous section, the $PSD_{output}(\xi)$ was determined in the following way:

For a given digitized frame of speckle data, a region of 500x500 pixels was selected. Each horizontal row of data is a single observation of an ergodic random process. A fast Fourier transform (FFT), which is a discrete Fourier transform, was performed on each row of speckle data. The magnitude squared in one dimension provided a single estimate of the one-dimensional power spectrum, $PSD_{output}(\xi)$. These 600 spectra were averaged, for a better signal-to-noise ratio in the $PSD_{output}(\xi)$ [23]. To reduce the noise even further, the average was taken for 10 frames.

The frames were stored in tiff format without compression, using an integration time of 0.050 s for the scientific CCD detector and 0.004 s for the CMOS detector. In the case of the video camera CCD detector, the frames were extracted in tiff format from a video recording captured with a rate of 25 frames/s for 1 s.

When a FFT is performed on a data set of length N, the Nyquist frequency appears at the N/2 component of the FFT output. A ratio can be formed to evaluate the spatial frequency ξ_n that corresponds to the n'th component as [20]:

$$\frac{\xi_{Ny}}{N/2} = \frac{\xi_n}{n} \tag{5}$$

Eq. (5) associates frequencies between zero and the Nyquist frequency with FFT components from 0 to the N/2 component. In this work we used N=1024, thus the total number of spatial frequencies contained in the range from 0 to the Nyquist frequency of the detector was 512.

Before processing, each digitized frame of speckle data was corrected in order to reduce effects from the spatial noise of the detector itself.

With respect to the spatial noise of a CCD, a distinction can be made between the fixed pattern noise (FPN) and the photoresponse non-uniformity (PRNU). The FPN refers to the pixel-to-pixel variation that occurs when the array is in the dark, and thus it is signal-independent noise. The PRNU is due to the difference of response of each pixel to a given signal; it is therefore signal-dependent noise.

The FPN was corrected by subtracting from the speckle image the dark image captured obscuring the detector, and the PRNU by means of the procedure proposed elsewhere [15].

For the processing of the speckle images, the appropriate software was developed using MATLAB.

Results and Discussion

For each wavelength analysed, the experimental values of the horizontal MTF of the detectors were calculated using Eq. (1).

For the three detectors, at each wavelength analysed, a polynomial fit of the experimental MTF values was made and the resulting functional expression was normalized by dividing it by the value that the adjustment equation provided at zero frequency.

The MTF experimental values of the detectors were normalized by dividing them by the same value used to normalize the corresponding adjustment curve (zero-order coefficient in the polynomial-fit expression).

The results are shown in Figures 2, 3, and 4, which reflect, for the different wavelengths of the visible spectrum, the experimental values of the horizontal MTF of each detector after normalization at zero spatial frequency. For greater clarity, all the points corresponding to the 512 MTF experimental values are not shown.

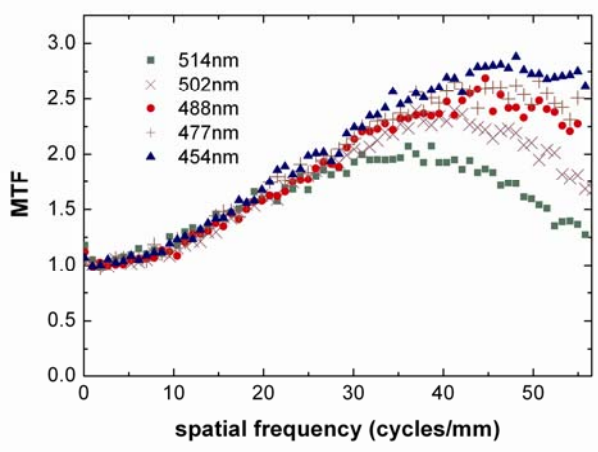

Figure 2. *MTF experimental values of the low-cost video camera CCD detector at different wavelengths of the visible spectrum.*

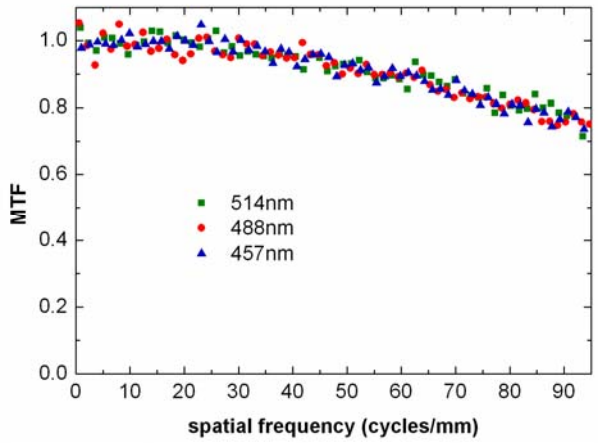

Figure 3. *MTF experimental values of the scientific camera CCD detector at different wavelengths of the visible spectrum.*

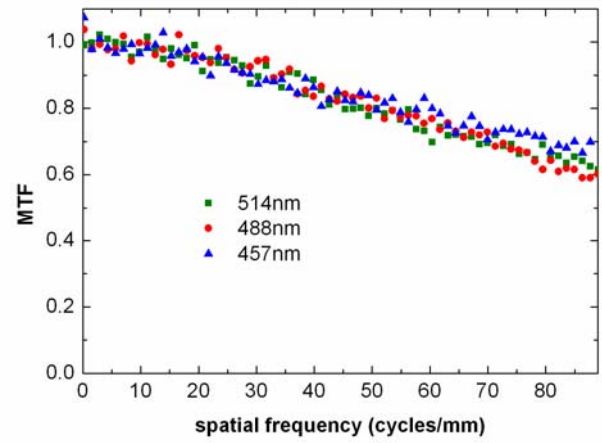

Figure 4. *MTF experimental values of the scientific camera CMOS detector at different wavelengths of the visible spectrum.*

In the case of the CCD video camera, considering that by definition the MTF is normalized at unity at zero spatial frequency, MTF values higher than one are reached due to the amplification introduced by the electronic filters of the image card [24, 25].

Figures 5, 6, and 7 show, for the three detectors and at the different wavelengths, the MTF curves given by the polynomial adjustments of the experimental values, after normalization at zero spatial frequency.

For each wavelength, the MTF curve of the low-cost video camera CCD detector was determined by fitting experimental values to a third-order polynomial function. The different correlation coefficients associated with these fits are listed in Table 4.

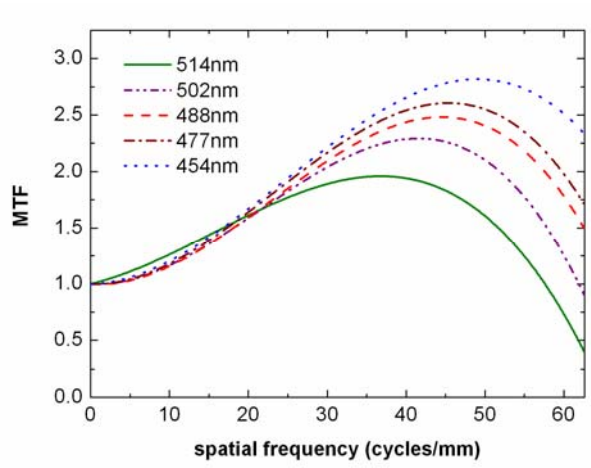

Figure 5. *MTF of the low-cost video camera CCD detector at different wavelengths of the visible spectrum. Curves were determined by fitting experimental values to a third-order polynomial function.*

Table 4: Correlation coefficients of fitting curves shown in Figure 5

Wavelength (nm)	Correlation coefficient
514	0.9847
502	0.9929
488	0.9947
477	0.9954
454	0.9958

At the different wavelengths, MTF curves of the scientific camera CCD detector were determined by fitting experimental values to a second-order polynomial function. The correlation coefficient corresponding to each of these adjustments is indicated in Table 5.

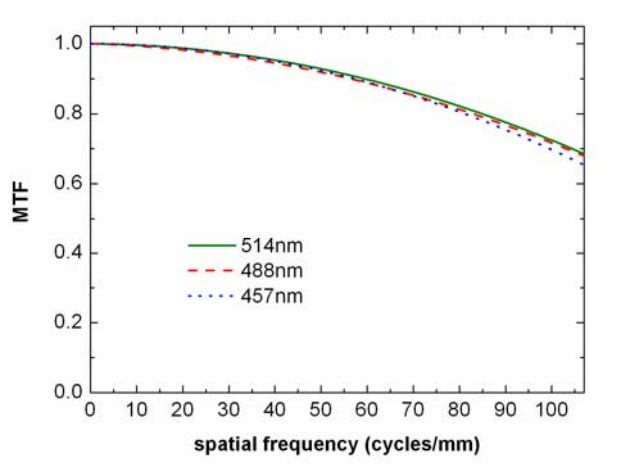

Figure 6. *MTF of the scientific camera CCD detector at different wavelengths of the visible spectrum. Curves were determined by fitting experimental values to a second-order polynomial function.*

Table 5: Correlation coefficients of fitting curves shown in Figure 6

Wavelength (nm)	Correlation coefficient
514	0.9646
488	0.9717
457	0.9727

For the scientific camera CMOS detector, MTF curves were determined by fitting experimental values to a third-order polynomial function at each wavelength. The correlations coefficients associated with these polynomial fits are shown in Table 6.

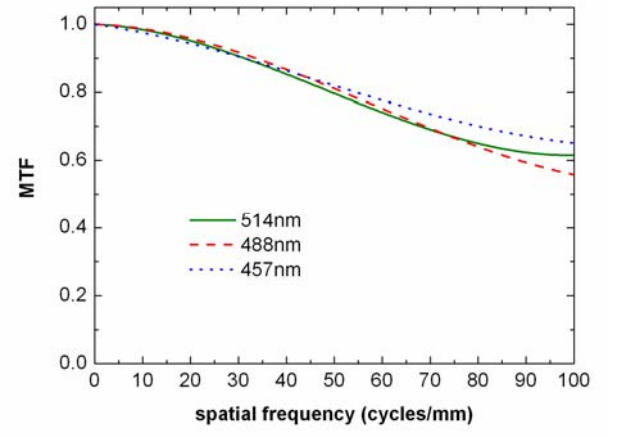

Figure 7. *MTF of the scientific camera CMOS detector at different wavelengths of the visible spectrum. Curves were determined by fitting experimental values to a third-order polynomial function.*

Table 6: Correlation coefficients of fitting curves shown in Figure 7

Wavelength (nm)	Correlation coefficient
514	0.9904
488	0.9913
457	0.9819

The comparison of the results show the differences between the cameras analysed with respect to the performance of the MTF of the detector with wavelength, within the spectral range studied.

For the CCD detector of the video camera, the highest value of the MTF was reached at the lowest of the wavelengths studied. The value of the spatial frequency for which the maximum of the MTF curve is found diminishes as the wavelength augments. Furthermore, the differences between the MTF curves corresponding to the different wavelengths analysed become more notable as the spatial frequency increases.

In the case of scientific cameras, the behaviour of the MTF with wavelength does not present the same trend as that observed for the low-cost video camera. Except at spatial frequencies close to the Nyquist frequency, for the CCD and CMOS detectors, no significant differences are appreciated in the MTF curves resulting at the different wavelengths, within the range of the visible spectrum studied.

For each of the three wavelengths studied, the CCD detector presented MTF values higher than those of the CMOS detector.

Differences in the MTF spectral behaviour of the two CCD detectors could be due to the effect of charge diffusion between pixels, which depends on wavelength [24]. Probably, the charge diffusion effect is greater for the low-cost CCD video camera, and therefore wavelength influences the MTF more significantly. In the case of the video camera, the horizontal MTF values are also affected by the electronic filters of the image card [11, 25].

For both scientific detectors, the overall MTF behaviour is determined by the pixel active area geometrical shape and the physical diffusion effect [24, 26]. The diffusion component of the MTF is due to the penetration depth of photons in the substrates and, as the wavelength increases, photon absorption occurs at increasing depths in the detector material [24, 26]. It is therefore expected that the MTF of the scientific detectors changes more clearly at longer wavelengths than those analysed in the present work.

Conclusions and Future Work

In this work, we have comparatively analysed the quality of the images provided by different detector arrays using the speckle method. In addition, we have compared their performance with wavelength within a range of the visible spectrum. For this, we have studied the MTF at several visible wavelengths, for the detectors of a low-cost CCD video camera and of two scientific cameras (a CCD and a CMOS).

Our results reveal differences in the MTF spectral-variation of the detector arrays analysed within the spectral range studied.

For the CCD detector of the video camera, the highest value of the MTF was reached at the lowest of the wavelengths studied. Also, the differences between the MTF curves corresponding to the different wavelengths become more notable as the spatial frequency increases.

In the case of scientific cameras, except at spatial frequencies near the Nyquist frequency, no significant differences are appreciated in the MTF of the detector at the different wavelengths, within the range studied.

Moreover, results prove the scientific CCD detector presented MTF values higher than those of the CMOS detector at the same spatial frequencies, for each of the three visible wavelengths analysed.

With the CCD video camera, the MTF reached values higher than one due to the amplification introduced by the electronic filters of the image card.

Since the penetration depth of photons in the detector material increases with the wavelength, effects of smear and signal loss are more pronounced at higher wavelengths. Therefore, the influence of the diffusion on the MTF of the detector is stronger as the wavelength increases. In this sense, it would be worthwhile to carry out new measurements at higher wavelengths than those analysed here.

At the moment, we are interested in extending the present work to study the MTF spectral-variation of different detector arrays at higher wavelengths within the visible spectrum.

Acknowledgements

The authors express their appreciation to the Ministerio de Ciencia y Tecnología of Spain for financing project FIS2004-06465-C02-02

References

[1] G. C. Holst and T. S. Lomheim, CMOS/CCD Sensors and Camera Systems (JCD Publishing, Winter Park, FL. and SPIE Optical Engineering Press, Bellingham, WA, 2007).

[2] H. Helmers and M. Schellenberg, “CMOS vs. CCD sensors in speckle interferometry”, Opt. Laser Technol., 35, 587–595 (2003).

[3] D. Litwiller, “CCD vs. CMOS: facts and fictions”, Photonics Spectra, 154–158 (2001).

[4] J. Janesick, “Dueling detectors. CMOS or CCD?”, SPIE’s OE Magazine, 41, 30-33 (2002).

[5] J. Janesick, “Lux transfer: complementary metal oxide semiconductors versus charge-coupled devices”, Opt. Eng., 41, 1203–1215 (2002).

[6] G. Deptuch, A. Besson, P. Rehak, M. Szelezniak, J. Wall, M. Winter and Y. Zhu, “Direct electron imaging in electron microscopy with monolithic active pixel sensors”, Ultramicroscopy, 107, 674–684 (2007).

[7] S. K. Park, R. Schowengerdt and M. Kaczynski, “Modulation-transfer-function analysis for sampled image system”, Appl. Opt., 23, 2572-2582 (1984).

[8] J. C. Feltz and M. A. Karim, “Modulation transfer function of charge-coupled devices”, Appl. Opt., 29, 717-722 (1990).

[9] D. N. Sitter, Jr., J. S. Goddard, and R. K. Ferrell, “Method for the measurement of the modulation transfer function of sampled imaging systems from bar-target patterns”, Appl. Opt., 34, 746-751 (1995).

[10] A. Daniels, G. D. Boreman, A. D. Ducharme, and E. Sapir, “Random transparency targets for modulation transfer function measurement in the visible and infrared regions”, Opt. Eng., 34, 860-868 (1995).

[11] S. M. Backman, A. J. Makynen, T. T. Kolehmainen, and K. M. Ojala, “Random target method for fast MTF inspection”, Opt. Express, 12, 2610-2615 (2004).

[12] N. Guérineau, J. Primot, M. Tauvy and M. Caes, “Modulation transfer function measurement of an infrared focal plane array by use of the self-imaging property of a canted periodic target”, Appl. Opt., 38, 631-637 (1999).
[13] M. Marchywka and D. G. Socker, “Modulation transfer function measurement techniques for small-pixel detectors”, Appl. Opt., 31, 7198-7213 (1992).
[14] J. E. Greivenkamp and A. E. Lowman, “Modulation transfer function measurements of sparse-array sensors using a self-calibrating fringe pattern”, Appl. Opt., 33, 5029-5036 (1994).
[15] A. M. Pozo, A. Ferrero, M. Rubiño, J. Campos and A. Pons, “Improvements for determining the modulation transfer function of charge-coupled devices by the speckle method”, Opt. Express, 14, 5928-5936 (2006).
[16] G. D. Boreman and E. L. Dereniak, “Method for measuring modulation transfer function of charge-coupled devices using laser speckle”, Opt. Eng., 25, 148-150 (1986).
[17] A. D. Ducharme, "Microlens diffusers for efficient laser speckle generation", Opt. Express, 15, 14573-14579 (2007).
[18] G. D. Boreman, Y. Sun and A. B. James, “Generation of laser speckle with an integrating sphere”, Opt. Eng., 29, 339-342 (1990).
[19] M. Sensiper, G. D. Boreman, A. D. Ducharme and D. R. Snyder, “Modulation transfer function testing of detector arrays using narrow-band laser speckle”, Opt. Eng., 32, 395-400 (1993).
[20] A. M. Pozo and M. Rubiño, “Comparative analysis of techniques for measuring the modulation transfer functions of charge-coupled devices based on the generation of laser speckle”, Appl. Opt., 44, 1543-1547 (2005).
[21] J. W. Goodman, Statistical properties of laser speckle and related phenomena, in Laser Spekle and Related Phenomena, (J. C. Dainty, Ed., Vol. 9 of Topics in Applied Physics Springer-Verlag, Berlin, 1984), pg. 35-40.
[22] L. I. Goldfischer, “Autocorrelation function and power spectral density of laser-produced speckle patterns”, J. Opt. Soc. Am., 55, 247-253 (1965).
[23] G. D. Boreman, “Fourier spectrum techniques for characterization of spatial noise in imaging arrays”, Opt. Eng., 26, 985-991 (1987).
[24] G. C. Holst, CCD Arrays, Cameras and Displays, (JCD Publishing, Winter Park, FL. and SPIE Optical Engineering Press, Bellingham, WA, 1996).
[25] B. T. Teipen and D. L. MacFarlane, “Liquid-crystal-display projector-based modulation transfer function measurements of charge-coupled-device video camera systems”, Appl. Opt., 39, 515-525 (2000).
[26] I. Shcherback and O. Yadid-Pecht, CMOS APS MTF Modeling, in CMOS Imagers: From Phototransduction to Image Processing, (O. Yadid-Pecht and R. Etienne Cummings, Eds., Kluwer Academic, Norwell, MA, 2004), pg. 53-74.

Author Biography

Alicia Fernández-Oliveras received the B.S. degree in physics from University of Granada, Granada, Spain, in 2007 and she is pursuing the M.S. degree in physics. She currently collaborates with the Department of Optics, University of Granada, where she has developed several research contracts under project FIS2004-06465-C02-02, financed by the Spanish Ministry of Education. She is engaged in the research, development, and applications of measurement methods to evaluate image quality of CCD and CMOS arrays systems.

Antonio M. Pozo received the B.S. and M.S. degrees in physics from University of Granada, Granada, Spain, in 2000 and 2003, respectively, where he is also a graduate in optics and optometry. He is an associate professor with the Department of Optics in the Science Faculty, University of Granada. He has been conducting research in experimental methods to evaluate image quality of systems based on CCD and CMOS detectors, publishing several papers in these fields.

Manuel Rubiño received his M.S. (1986) and Ph.D. in Physics (1990) from the University of Granada, Granada, Spain. Since then he has worked as an associate professor of Radiometry, Photometry, Colorimetry and Optical Technology in the Department of Optics at the University of Granada. His research interests are optical and radiometric characterization of CCD and CMOS cameras, applied Colorimetry and applied Photometry.